Appendix K
Earthquakes' Impact on Cable Tensions

1.0 Introduction

The island of Puerto Rico is in a seismically active region between the North American and Caribbean tectonic plates. As a result, the telescope has experienced multiple earthquakes since construction in 1963. In January 2020, less than a year before the telescope's collapse, Puerto Rico was hit by a series of significant earthquakes with magnitudes up to 6.4 (January 7, 2020).

This appendix presents our analysis of the seismic effects on the telescope's cable system. The objective is to determine how much tension and how many tension cycles the cables and sockets experienced during representative earthquakes.

2.0 Background

Between the completion of the original telescope in 1964 to the first cable failure in August 2020, there was approximately 200 earthquakes of magnitude greater than 4.5 within 125 miles of Arecibo Observatory (AO).

The subsurface conditions at the site consist of surficial clay and silt layers underlain by limestone. Consequently, tower and anchor foundations are generally supported on competent limestone, which is consistent with a site class C per ASCE 7-16. Based on measurements at various locations in Puerto Rico, the shear wave velocity is estimated to be between 1,475 and 2,065 foot per second (ft/s) at the AO site.

A seismic monitoring station is located at AO. Designated as AOPR, the station is part of the Puerto Rico Seismic Network and is located on a hill of similar subsurface conditions and topography as the where the telescope's towers and cable anchors are build. Therefore, ground motion recorded by the AOPR station is used input for our seismic analysis.

In early 2020, a sequence of earthquakes took place in the southwest region of Puerto Rico, with 43 events magnitude greater than 4.5 recorded before the first cable failure. The strongest earthquake happened on January 7, 2020, with a magnitude of 6.4 and and epicenter 29 miles south of AO at a depth of 4.3 miles. The second-largest earthquake was an aftershock on January 11, 2020, with a magnitude of 5.9 and an epicenter 28 miles south of AO at a depth of 3.1 miles. Both earthquakes were strongly felt at AO. Due to the relatively short time (eight months) between the two earthquakes and the first cable failure, it is natural to evaluate the impact of those earthquakes on the telescope's cable system. The two earthquakes are referred to as M6.4 and M5.9 in this appendix.

Figure 1 shows the acceleration time histories at the AOPR station for M6.4 and M5.9, with the corresponding acceleration response spectra. Also shown in the figure is the Design Earthquake (DE) response spectrum per the ASCE 7-16 standard[1] at the AO site for an assumed site class C. All spectra are based on five percent damping. The DE spectrum is about two times larger at shorter periods and about five times larger at moderate to long periods than the M6.4 earthquake. The 2020 earthquakes were therefore significantly less severe than the current design earthquake for the AO site.

[1] American Society of Civil Engineers (ASCE). *ASCE 7-16. Minimum Design Loads and Associated Criteria for Buildings and Other Structures*. Chapters 26 and 29. 2016.

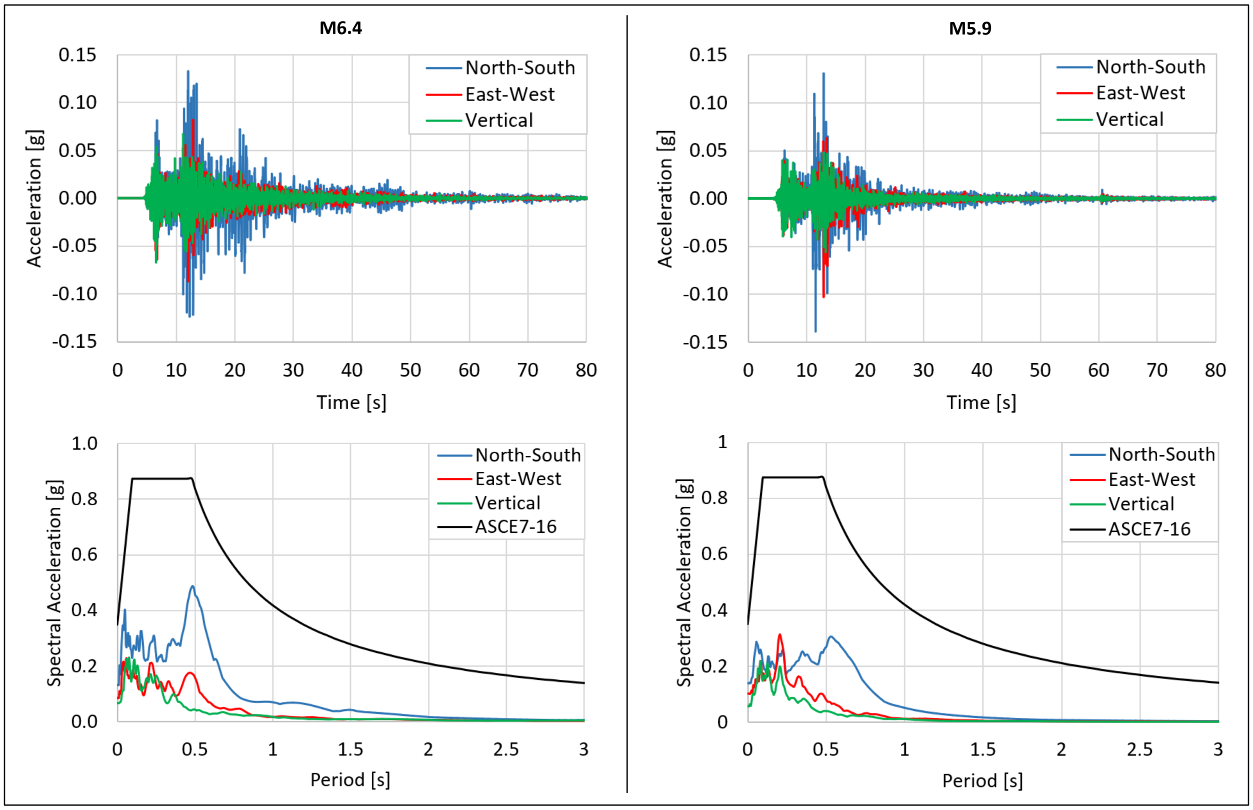

Figure 1: Ground acceleration time histories and five percent damping response spectra for M6.4 and M5.9 earthquakes.

3.0 Structural Response Analysis

To evaluate the potential impact of seismic activity on the telescope structure, we simulated the M6.4 and M5.9 earthquakes in finite element (FE) models of the original and upgraded telescope. The FE models are described in appendix F.

The ground accelerations of the M6.4 and M5.9 earthquakes were recorded by AO's seismic station (AOPR), and the towers and anchors of the telescope experienced similar accelerations. However, due to the distance between the different towers and cable anchors, the arrival time of the acceleration was slightly different at each tower and anchor location. The recorded ground accelerations were therefore applied to the FE models with time delays between towers and anchors calculated from the shear wave velocity at the site (Figure 2).

As shown in Table 1, a total of eight analyses were performed considering two structures (original and upgraded), two earthquakes (M6.4 and M5.9), and the two bounds of the shear wave velocity (1,475 ft/s and 2,065 ft/s).

The analyses use multi-support excitation to consider the propagation of ground motions to the different towers, anchorages, and tie-down cable supports. The acceleration times histories in three directions were converted to ground displacement time histories and applied to the FE models with time delays between towers and anchors calculated from the shear wave velocity at the site. Nonlinear direct integration time history was performed, with a Rayleigh damping model calibrated such that the effective damping ratio is one percent for the first two modes of the structure.

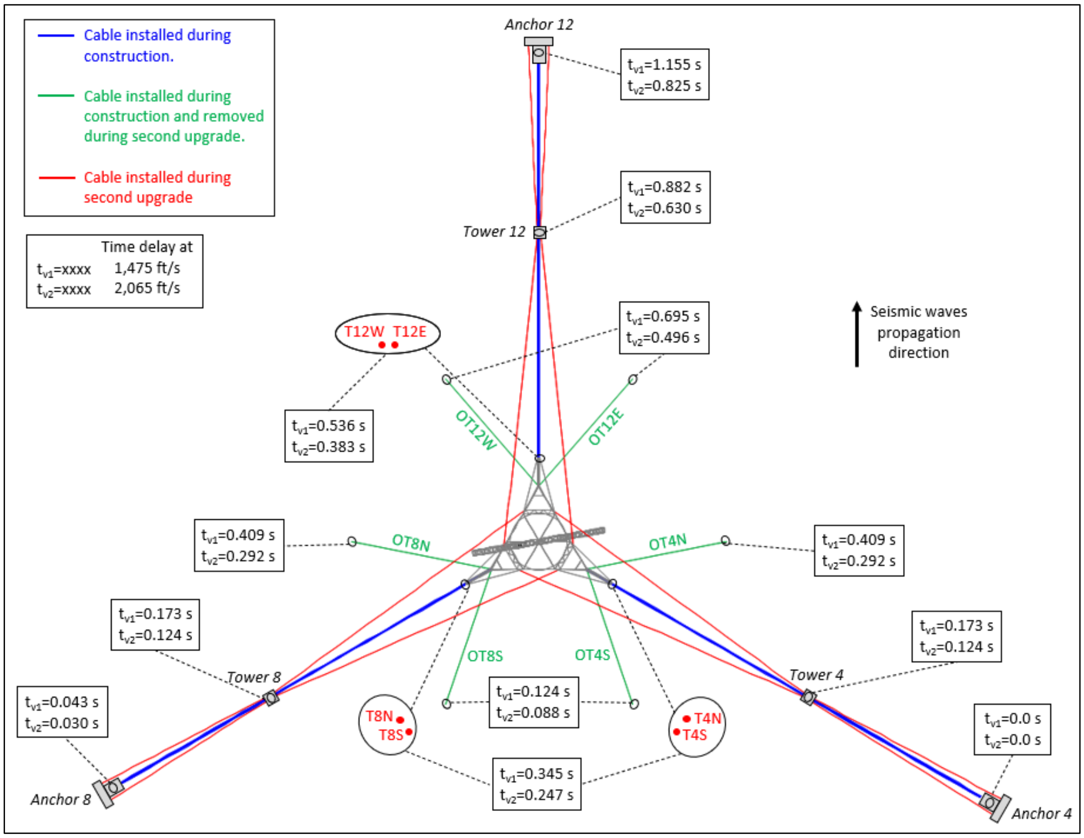

Figure 2: Ground motion time delay based on two shear wave velocities (1,475 and 2,065 ft/s).

Table 1: Earthquake analyses performed.

Analysis #	Telescope Model	Earthquake	Shear Wave Velocity [ft/s]
1	Upgraded	M6.4	1,475
2	Upgraded	M6.4	2,065
3	Upgraded	M5.9	1,475
4	Upgraded	M5.9	2,065
5	Original	M6.4	1,475
6	Original	M6.4	2,065
7	Original	M5.9	1,475
8	Original	M5.9	2,065

4.0 Cable Tension Results

4.1 Original Structure

The cable tension time histories in the original structure are shown in Figure 3 for the M6.4 and M5.9 earthquakes, with a shear wave velocity of 2,065 ft/s. The cable tension maps (Figure 4, Figure 5, and Figure 6) show the worst-case envelope over the four cases considered (M6.4 and M5.9 earthquakes, with 1,475 ft/s and 2,065 ft/s shear wave velocity).

Figure 4 shows the maximum tension increase in each cable during the earthquake as a percentage of the pre-earthquake tension. Excluding the tiedowns, the maximum tension increase is 10 percent and occurs in the backstays of Tower 8.

Figure 5 shows the lowest safety factor reached in each cable during the earthquake. The lowest safety factor is the ratio of the highest cable tension experienced during the earthquake to the cable’s minimum breaking strength. The safety factors remain around two in all of the cables.

Figure 6 shows the maximum normalized stress range experienced by each cable during the earthquake. The maximum normalized stress range is the ratio of the maximum tension range (difference between the maximum and minimum tension experienced) to the cable’s minimum breaking strength. The maximum normalized stress range is between two and nine percent in the mains and backstays.

Table 2 shows the number of stress cycles experienced by each cable during an earthquake for different stress levels. The number of cycles were counted in the cable tension time history results using the rainflow method, and averaged over the four cases considered (M6.4 and M5.9 earthquakes, with 1,475 ft/s and 2,065 ft/s shear wave velocity).

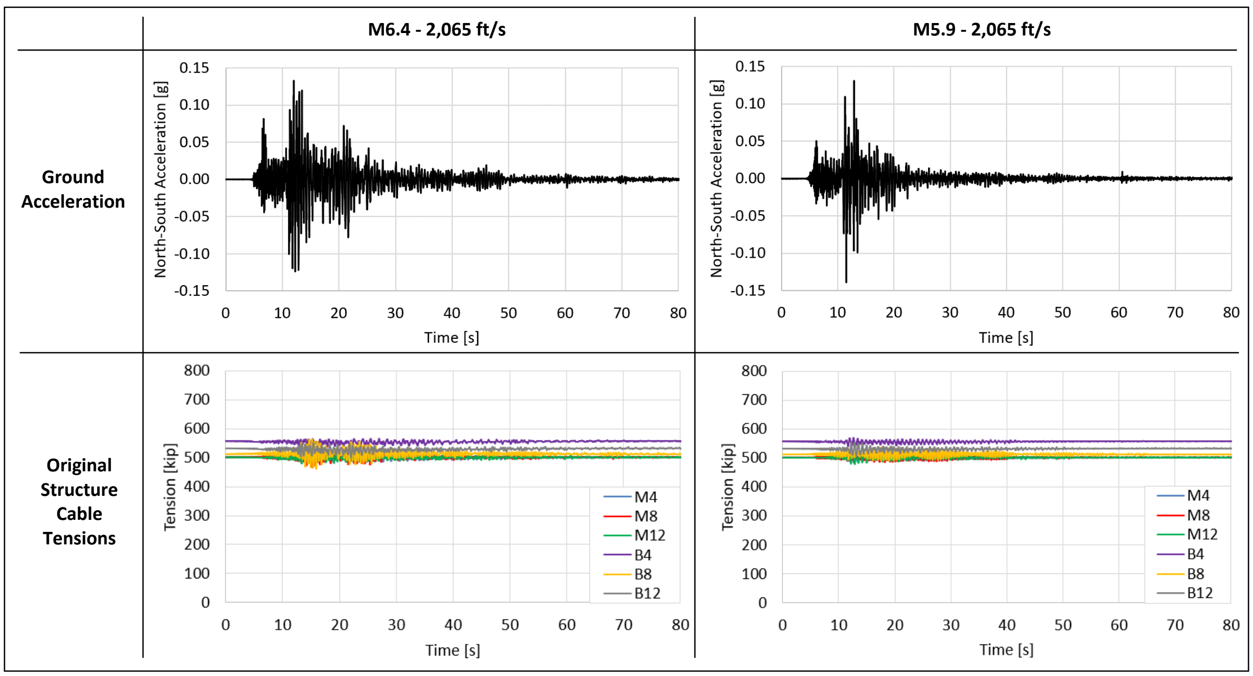

Figure 3: Cable tension time history in original structure during M6.4 and M5.9 earthquakes, with 2,065 ft/s shear wave velocity.

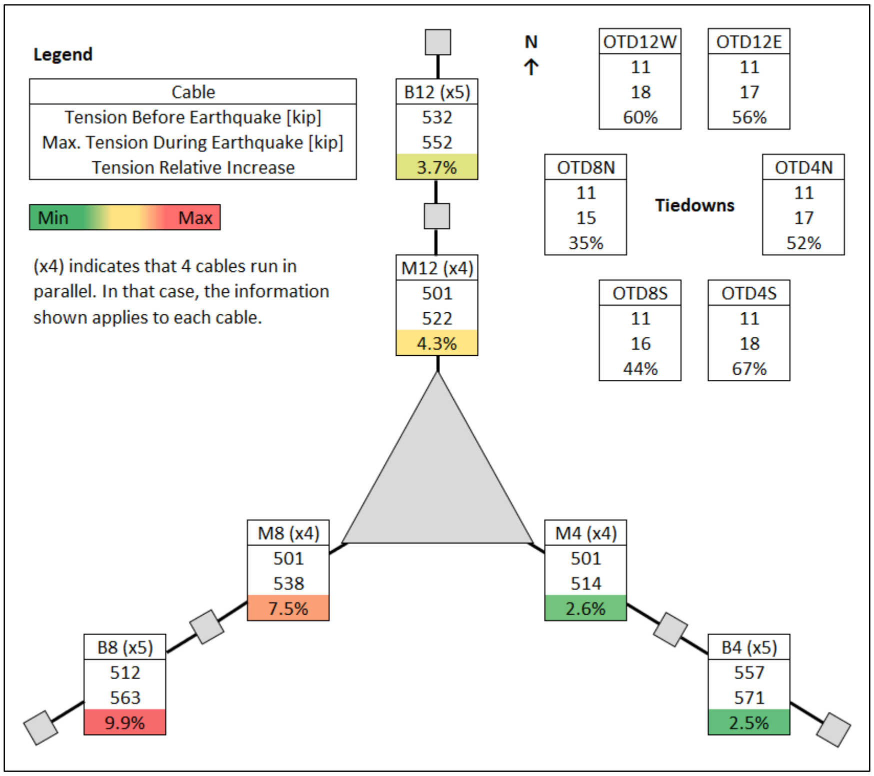

Figure 4: Maximum cable tension increase in original structure due to 2020 earthquakes.

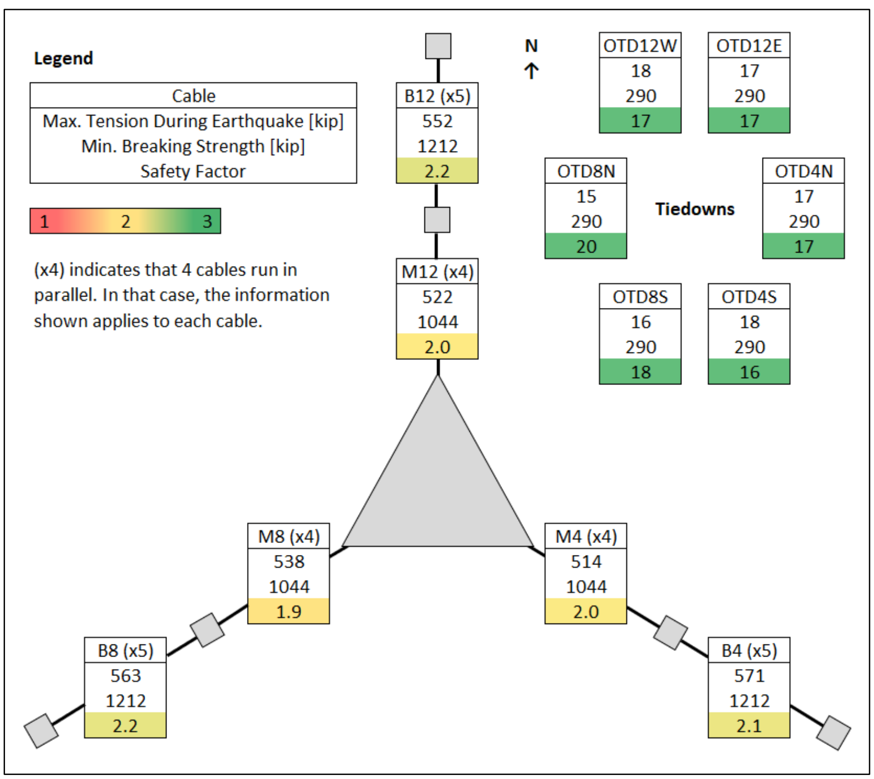

Figure 5: Maximum cable tension and corresponding safety factor in original structure due to 2020 earthquakes.

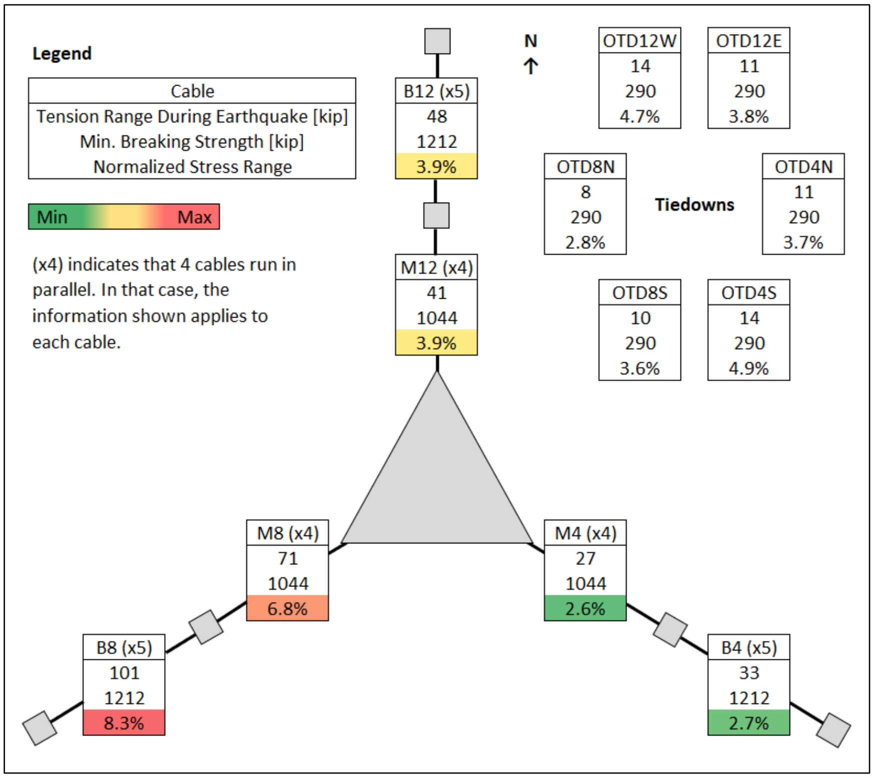

Figure 6: Maximum normalized stress range in cables of original structure due to 2020 earthquakes.

Table 2: Average number of stress cycles in cables of original structure during a 2020 earthquake.

	Normalized Stress Range (= Tension Range / Minimum Breaking Strength)							
	1-2%	**2-3%**	**3-4%**	**4-5%**	**5-6%**	**6-7%**	**7-8%**	**8-9%**
M4	21	2.3						
M8	16	8.5	7.0	4.5	1.3	0.5		
M12	17	6.8	1.8					
B4	17	1.3						
B8	21	11	7.5	4.8	3.3	2.3	1.5	0.3
B12	18	6.8	1.8					

4.2 Upgraded Structure

The cable tension time histories in the original structure are shown in Figure 7 for the M6.4 and M5.9 earthquakes with a shear wave velocity of 2,065 ft/s. The cable tension maps (Figure 8, Figure 9, and Figure 10) show the worst-case envelope over the four cases considered (M6.4 and M5.9 earthquakes, with 1,475 ft/s and 2,065 ft/s shear wave velocity).

Figure 8 shows the maximum tension increase in each cable during the earthquake as a percentage of the pre-earthquake tension. The maximum tension increase is five percent, occurring in the M12 main cables.

Figure 9 shows the lowest safety factor reached in each cable during the earthquake. The lowest safety factor is the ratio of the highest cable tension experienced during the earthquake to the cable's breaking strength. The safety factors in the mains and bactays are around or above two, and the safety factor in cable M4N (first cable failure) is 2.1.

Figure 10 shows the maximum normalized stress range experienced by each cable during the earthquake. The maximum normalized stress range is the ratio of the maximum tension range (difference between the maximum and minimum tension experienced) to the cable's breaking strength. The maximum normalized stress range is between two and five in the mains and backstays.

Table 3 shows the number of stress cycles experienced by each cable during the earthquake for different stress levels. The number of cycles were counted in the cable tension time history results using the rainflow method, and averaged over the four cases considered (M6.4 and M5.9 earthquakes, with 1,475 ft/s and 2,065 ft/s shear wave velocity).

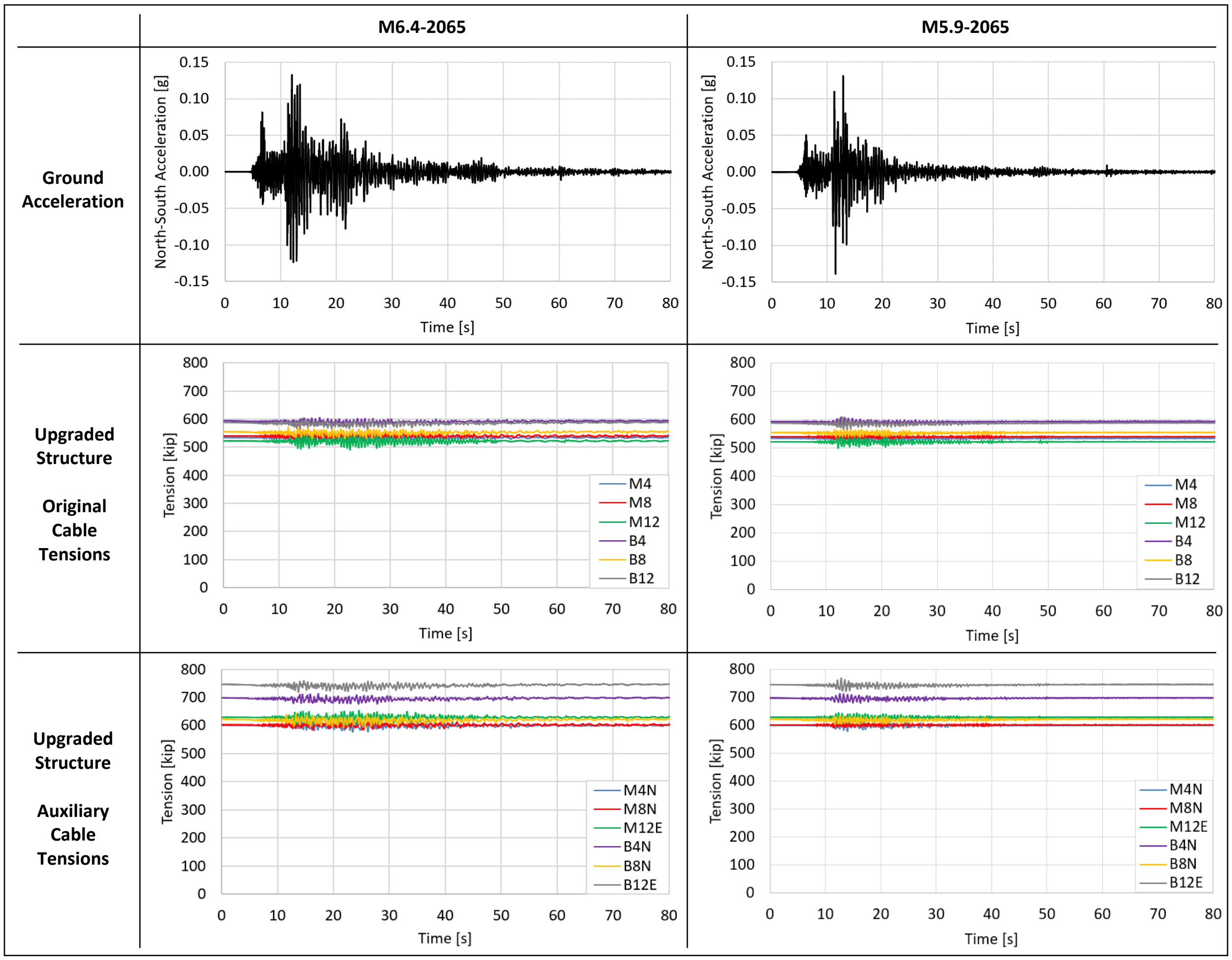

Figure 7: Cable tension time history in original structure during M6.4 and M5.9 earthquakes, with 2,065 ft/s shear wave velocity.

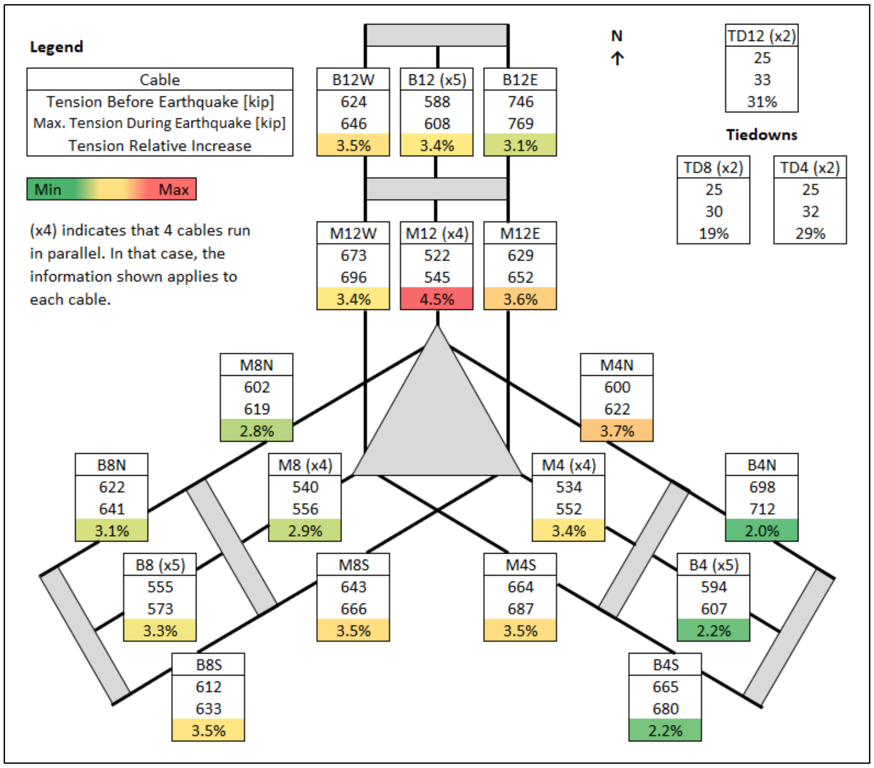

Figure 8: Maximum cable tension increase in upgraded structure due to 2020 earthquakes.

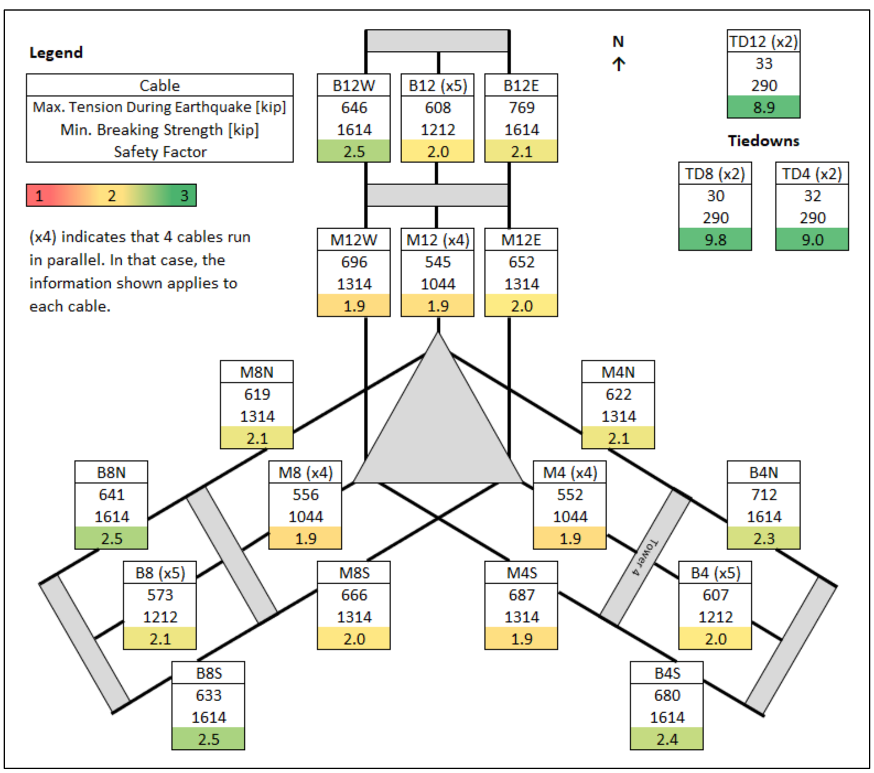

Figure 9: Maximum cable tension and corresponding safety factor in upgraded structure due to 2020 earthquakes.

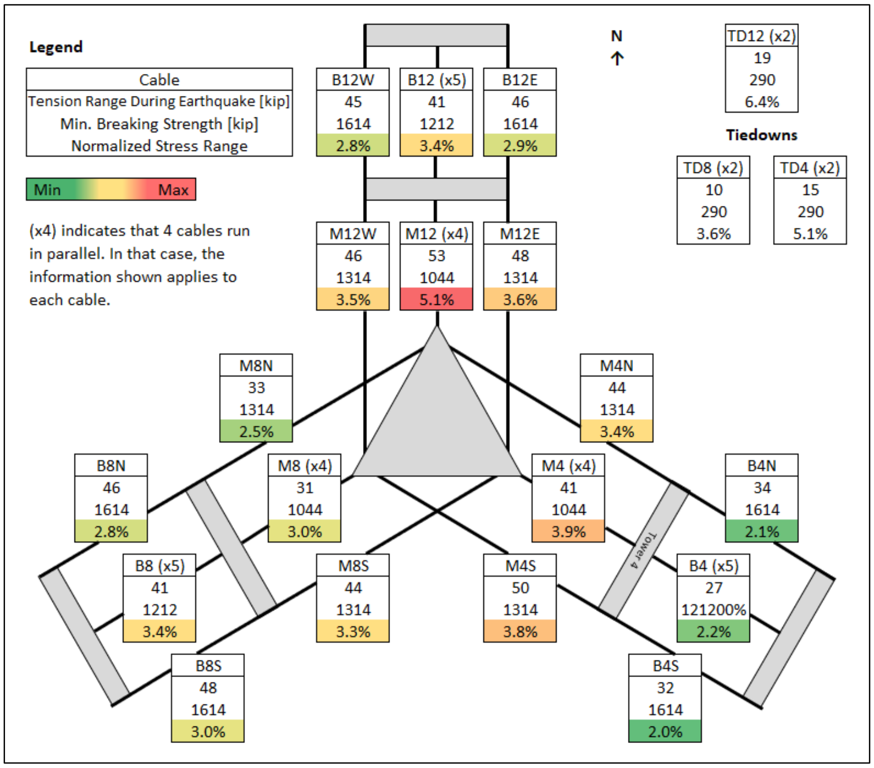

Figure 10: Maximum normalized stress range in cables of upgraded structure die to 2020 earthquakes.

Table 3: Average number of normalized stress cycles in cables of upgraded structure during a 2020 earthquake.

	Normalized Stress Range (= Tension Range / Breaking Strength)				
	1-2%	**2-3%**	**3-4%**	**4-5%**	**5-6%**
M4	22	8.0	0.8		
M4N	23	3.3	0.8		
M4S	16	3.3	0.8		
M8	19	4.0			
M8N	15	1.5			
M8S	15	5.8	0.5		
M12	28	14	8.3	2.3	0.3
M12E	21	10	2.8		
M12W	21	7.3	1.8		
B4	14	0.8			
B4N	11	0.3			
B4S	11				
B8	28	6.8	1.5		
B8N	22	4.5			
B8S	22	5.0			
B12	20	4.8	0.3		
B12E	18	2.3			
B12W	20	2.0			